Mechanistic Investigation of a Dual Bicyclic Photoinitiating System for Synthesis of Organic–Inorganic Hybrid Materials

Julien Christmann, Suqing Shi, Ahmad Ibrahim, Christian Ley, Céline Croutxe-Barghorn, Marjolaine Bessières, Xavier Allonas

Mechanistic Investigation of a Dual Bicyclic Photoinitiating System for Synthesis of Organic – Inorganic Hybrid Materials

*Julien Christmann, Suqing Shi†, Ahmad Ibrahim, Christian Ley, Céline Croutxé-Barghorn, Marjolaine Bessières, Xavier Allonas**

Laboratory of Macromolecular Photochemistry and Engineering, University of Haute-Alsace, 3b rue Alfred Werner 68093 Mulhouse, France

Keywords:

Photocyclic initiating system; dual-cure polymerization; cationic polymerization, free radical polymerization; photoacid generator

Abstract

One-pot synthesis of organic – inorganic hybrid materials under light requires specific photoinitiating systems which are able to release several different initiating species after light absorption. In this paper, the reaction mechanism of a photocyclic three-component initiating system based on isopropylthioxanthone as photoinitiator, an iodonium salt and a thiol as co-initiators was studied. It is shown that this system enables simultaneous release of both radicals and protons which are able to initiate respectively a free radical photopolymerization and the hydrolysis-condensation of a sol-gel network. Time-resolved investigations by Laser Flash Photolysis show that the initiating species are produced within two concomitant cyclic reaction mechanisms depending on the relative quantities of the co-initiators. Protons resulting from the secondary dark reaction of a photocyclic system are detected for the first time at the microsecond scale by means of a proton-sensitive molecular probe and corresponding quantum yields are measured. Finally, synthesis of organic, inorganic and hybrid materials under LED light at 395 nm is evaluated with respect to the mechanistic considerations demonstrating the dual initiating character of the system.

Introduction

Following the pioneering work of G. Ciamician[1], light is nowadays a significant sustainable energy source for the triggering of chemical processes, especially material synthesis. Light offers several major advantages over classic thermal sources, such as spatial and temporal control, ease of use, cost reduction, room temperature process… Polymeric materials can be easily synthesized under light using various processes such as free radical photopolymerization (FRP)[2-8], cationic ring opening photopolymerization[2-7,9-12], anionic photopolymerization[4-5,7,13], thiol-ene step growth reaction[14-15], photoclick polymerization[16-17] or hybrid organic-inorganic curing[18-22]. Several types of photoinitiating systems (PISs) have been developed in order to optimize the conversion of light into chemical energy and to improve the initial quantum yield in reactive species.[2-33]

Among the materials formed under light, organic/inorganic hybrid materials present interesting properties due to the elegant combination of the properties of organic polymers and inorganic materials through the *in-situ* formation of interpenetrated network or generation of chemical bonds between organic and inorganic components.[18-22] They are conventionally synthesized through a two-step process: a first sol-gel thermal reaction produces a liquid organic based polysilicate network which is further photopolymerized, leading to a solid cross-linked hybrid system. Beside this approach, an innovative process has been proposed in which a concomitant organic-inorganic photopolymerization occurs in a one-step water- and solvent free approach. UV light triggers the generation of acids or bases capable of catalyzing simultaneously both sol-gel reaction and organic photopolymerization.[34-37] The fabrication of such hybrid materials generally involves both the photopolymerization of multifunctional (meth)acrylates or epoxides, and the photocatalyzed hydrolysis-condensation of metal alkoxide inorganic precursors (i.e. alkoxysilanes). In most cases,

the widely available (meth)acrylate monomers (or oligomers) and free radical photoinitiators make poly(meth)acrylates-based hybrid materials much more attractive in the photocuring field. As a matter of course, the photoinitiating system responsible for simultaneous generation of radical and proton initiating species becomes definitely essential in the design and synthesis of poly(meth)acrylates-based hybrid materials.

Due to the lack of light absorption in the visible light region, the photoacid generator which is often an iodonium or sulfonium salt, seems to be the limits for developing poly(meth)acrylates-based hybrid materials under more environmental and sustainable light (i.e. visible light LEDs). Recently, a visible light photoacid generator with fast protonic acid release behavior has been reported by combining isopropylthioxanthone (ITX) with an iodonium salt (IOD^+).[37] The addition of a thiol (RSH) to a blend of ITX and IOD^+ is able to initiate simultaneously the free radical photopolymerization of dimethacrylates and the cationic polymerization of epoxides under visible light LED with high monomer conversion rates.[27] This innovative three-component photoinitiating system is very promising to design and prepare poly(meth)acrylate-based organic-inorganic hybrid materials. Nevertheless, the photochemical mechanism for efficient production of radical and protonic acid initiating species by photolysis of this three-component photoinitiating system is still unclear up to now. The aim of this paper is to understand the photochemical mechanism of this innovative dual-mechanistic photoinitiating system by Laser Flash Photolysis. Primary photoreactions of ITX with either IOD^+ or RSH are first studied. The resulting ITX photoproducts are found to be involved in secondary dark reactions with these co-initiators, leading to additional formation of reactive species such as radicals that are evidenced by LFP. The photogenerated protons are detected at the microsecond scale for the first time with a proton-sensitive molecular probe and the proton production quantum yield is also calculated. These mechanistic

considerations are finally correlated to the synthesis results of poly(meth)acrylates, polysiloxane and the corresponding hybrid materials.

Experimental and Theoretical Methods

Isopropylthioxanthone (ITX) purchased from Fluka was a mixture of 2- and 4-isopropylthioxanthone (75% and 25%, respectively, as checked by ^{1}H-NMR). Quinine sulfate dihydrate (98%) was purchased from Sigma. Pentaerythritol tetrakis(3-mercaptopropionate) (RSH, 95%) was supplied by Aldrich. Cumenyl(tolyl)iodonium tetrakis(pentafluorophenyl) borate (IOD^{+}, 98%) was obtained from TCI. Acetonitrile (99.97%) was got from Biosolve. Ethoxylated (3) bisphenol A dimethacrylate (SR348C) was provided by Sartomer. Poly(dimethoxysiloxane) (PDMOS) is a non-hydrolyzed oligomeric silicate precursor obtained from ABCR. Further information concerning PDMOS structure can be found elsewhere.[36] All chemicals were used as received. Their structures are presented in Chart 1.

Chart 1. Molecular structures of the compounds used in this study.

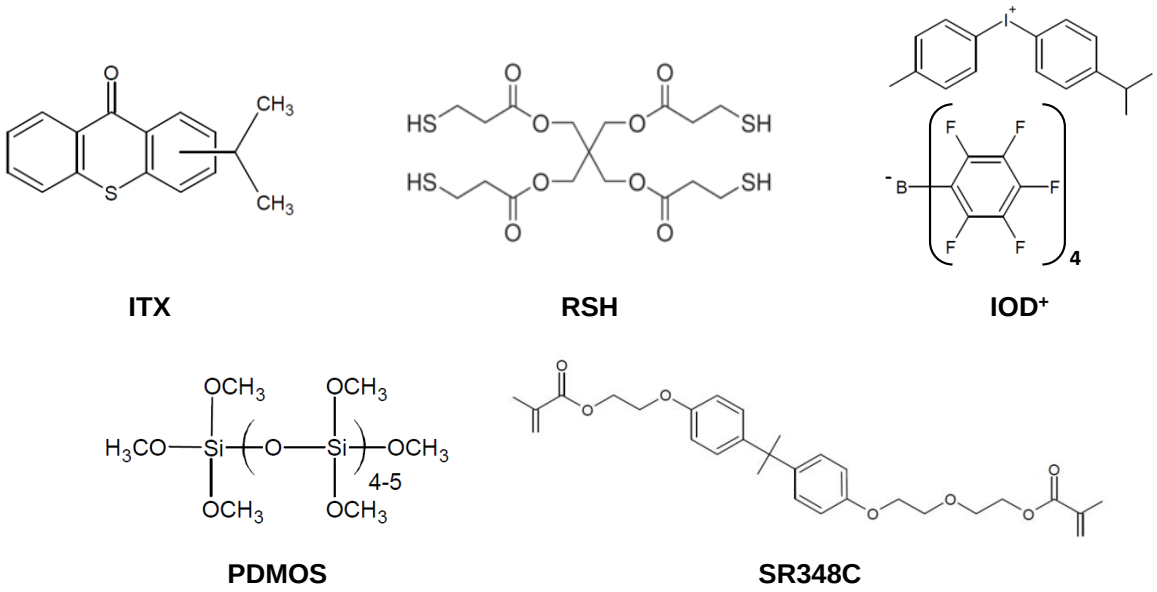

Absorption and fluorescence spectra were recorded at room temperature with an Analytik Jena Specord 210 UV-visible spectrometer and a Horiba Jobin Yvon Fluoromax 4 spectrofluorimeter respectively. Compounds were dissolved in acetonitrile and placed into 1 cm × 1 cm quartz cuvette. The fluorescence quantum yield (Φ_{fluo}) of ITX was determined with quinine sulfate dihydrate in 1N H_2SO_4 as reference ($\Phi_{fluo} = 0.546$[38]), using a conventional procedure.[39] Maximal optical density above 300 nm was maintained below 0.1 in order to avoid inner filter effects. Two excitation wavelengths (360 and 375 nm) and two slit sizes (1 and 2 nm) were used and the results were averaged on these four experiments.

Fluorescence lifetime of ITX was obtained by Time-Correlated Single Photon Counting (TCSPC) using a Horiba Jobin Yvon Fluoromax 4 spectrofluorimeter equipped with a Horiba Jobin Yvon Fluorohub module. Light source was ensured by a Horiba Jobin Yvon 374 nm nano-

LED (< 200 ps) and maximal optical density above 300 nm was also maintained below 0.1. Samples were previously deaerated by argon bubbling (15 min).

The relaxed triplet state energy of ITX was calculated in the same manner as reported elsewhere[40-41]. Redox potentials were determined by cyclic voltammetry, as described in Ref 42.

Nanosecond transient absorption experiments were realized with an Edinburgh transient absorption spectrometer. It combines a 50 W xenon lamp (Xe 900), a TM300 monochromator and a photomultiplier tube monitored by a digital oscilloscope. Light excitation was ensured by the third harmonic (355 nm) of a Continuum Powerlite 9010 Nd:YAG pulsed laser operating at 10 Hz.[43] Optical density of the solution was set at 0.10 for quenching and 0.55 for other experiments at the excitation wavelength. Incident intensity was set around 4-5 mJ/pulse for transient absorption spectra recording and ITX triplet state quenching analysis, and 10 mJ/pulse for the other experiments. Solutions were previously saturated with argon (15 min) in order to eliminate molecular oxygen. Quenching rate constants (k_q) were obtained by the usual Stern-Volmer treatment:

$$\tau^{-1} = \tau_0^{-1} + k_q[Q] \qquad \text{Eq. 1}$$

τ and τ_0, respectively, refer to the triplet state lifetime with and without any quencher Q. [Q] is the concentration of this quencher in the cell.

Photoacid production quantum yield (Φ_{H+}) was estimated by a spectroscopic method using Quinaldine Red (QR) as an acid sensor in a similar way to that already reported.[44] Three-component systems were dissolved in acetonitrile where a small amount of QR was added. The obtained solution was then irradiated by the Powerlite 9010 pulsed laser at 355 nm (absorption by

the other compounds was neglected at their respective concentrations). The absorbed light energy (E_{abs}) was calculated with the following equation:

$$E_{abs} = I_0 \int_0^t (1 - 10^{-OD(t)})dt \quad \text{Eq. 2}$$

and

$$OD(t) = \varepsilon_{355}^{ITX}.[ITX](t).l \quad \text{Eq. 3}$$

I_0 is the incident light intensity (in mJ/pulse). ε_{355}^{ITX} stands for the molar extinction coefficient of ITX at 355 nm, [ITX](t) the concentration of ITX at each irradiation time t and l the optical path length of the cuvette containing the solution. The incident energy was maintained at 10 mJ/pulse during all the experiments. Preliminary experiments showed that ITX was not photolyzed by the number of pulses required in our study. The number of absorbed photons N_{abs} was then deduced from the ratio between the incident energy and that of one photon at 355 nm. The number of generated protons $N_{protons}$ was monitored through the decrease of the 520 nm band of QR, assuming a quantitative relation between QR disappearance and H^+ production in the considered range. Finally, quantum yield was calculated as the ratio of these two quantities (Eq. 4). Results were averaged on three repetitions and the associated standard deviation was estimated.

$$\Phi_{H+} = \frac{N_{protons}}{N_{abs}} \quad \text{Eq. 4}$$

ITX based photoinitiating systems were used to trigger the free radical photopolymerization and the sol-gel process. The concentration of ITX was 2.5 mol% with respect to the monomer and/or organic precursor. For two-component systems, 1.5 mol% of co-initiator (IOD^+ or RSH) was contained. For three-component systems, 1.5 mol% of co-initiator (IOD^+ or RSH) and 0.15 mol% of another component (RSH or IOD^+, respectively) were both incorporated. To prepare the hybrid

materials, a mixture of PDMOS (80 mol%) and SR348C (20 mol%) was used and all other mol% were calculated on the basis of the total amount of PDMOS and SR348C.

Photopolymerization kinetics and monomer conversions were followed by real-time FTIR spectroscopy using a Vertex 70 from Bruker Optics operating in a rapid scan mode and being equipped with a nitrogen liquid cooled MCT detector.[45-46] The sampling interval was 0.1 s and the resolution was 4 cm^{-1}. The irradiation was provided by a 395 nm LED device (Roithner LaserTechnik) at 20 $mW.cm^{-2}$ under air. The intensity of the LED was measured using a calibrated fiber optic spectrometer (Ocean Optics, USB4000). The photopolymerization reaction was carried out under air at room temperature, using polypropylene film and BaF_2 pellet. Room humidity was kept constant at almost 43 – 45% by a hygrometer and consistent with previous work.[37] Each experiment was repeated at least three times to ensure a good reproducibility. Conversion of SR348C was followed by the decrease of the area of its twisting vibration band at 1310 cm^{-1} and calculated from:

$$\text{Conversion (\%)} = \frac{A_0 - A_t}{A_0} \times 100 \qquad \text{Eq. 5}$$

A_0 and A_t represent respectively the absorption band area before exposure and at exposure time t. Areas were corrected with a reference band (at 1510 cm^{-1}) in order to avoid any error from displacement of the 1310 cm^{-1} band. The absorbance decrease of the CH_3 symmetric stretching vibration band centered at 2848 cm^{-1} (distinctive from CH_3 methanol vibration modes) was monitored to follow the methoxysilyl hydrolysis ratio in PDMOS. The maximum rate of conversion R_c^{max} was determined as the maximum of the first derivative of the conversion with time.

Results and Discussion

Isopropylthioxanthone (ITX) has been considered as one of the most important photoinitiator in the field of photopolymerization.[33] It has been reported to act as both efficient photosensitizer for iodonium salts to trigger the cationic polymerization or sol-gel process, and effective type II photoinitiator for free radical polymerization, owing to its attracting photochemical and redox properties. Table 1 shows the photochemical and redox properties of ITX which were found very close to those reported in the literature.[47-57] Due to the known short lifetime of the first excited singlet state (τ_S) and the high intersystem quantum yield (Φ_{ISC}), ITX is expected to react from its lower triplet state which can be detected using laser flash photolysis. The transient absorption spectrum of ITX in argon saturated acetonitrile (Figure S1) exhibits a photobleaching at 385 nm and two peaks at 310 and 640 nm corresponding to the triplet – triplet absorption.

Table 1. Photochemical and redox properties of ITX in acetonitrile.

Properties	Present work	Literature	Properties	Present work	Literature
λ_{abs}^{max} (^{0}ITX) (nm)	383	386[47a]; 382[48-50]; 383[51]; 384[52]	λ_{abs}^{max} (^{3}ITX) (nm)	310, 630 – 640	605[51c]; 630[47a]; 635[54]; 640[52,55-56]; 650[50]
$\varepsilon(\lambda_{abs}^{max})$ ($L.mol^{-1}.cm^{-1}$)	5,600	5200[50]; 5300[48]; 6900[47a]; 6920[49]	Φ_T[d]	/	0.85 ± 0.1[47a]
λ_{em}^{max} (nm)	415	415[48]; 420[53]	E_T (eV)[d]	2.71[e]	2.64[55]; 2.66[51]; 2.71[54]
Φ_{fluo}	0.011	0.013[53]	τ_T (μs)[d]	4 – 5	3 – 4 [56]
E_S (eV)[b]	3.13	3.11[50]; 3.57[53]	$k_q^{3ITX/O2}$ ($L.mol^{-1}.s^{-1}$)[f]	/	4.8×10^9 [52]
τ_S (ps)[b]	280	200[53]	$E_{ox/red}$ / SCE (V)	1.51 / -1.73	1.54 / -1.63[57] - / -1.596[52g]

a. in benzene. b. "S" refers to the first excited singlet state. c. in methanol. d. "T" refers to the lowest triplet state. e. calculated by quantum mechanics. f. quenching rate constant of the reaction $^3ITX + O_2$. g. *vs.* AgCl.

ITX / IOD^+ as primary photoreaction

The reaction of ITX triplet state (^{3}ITX) with strong electron acceptors such as iodonium salts should result in ITX radical cation ($ITX^{\bullet+}$). Therefore, the photoinduced electron transfer reaction between ^{3}ITX, cumenyl(tolyl)iodonium tetrakis(pentafluorophenyl)borate (IOD^+, Chart 1) was firstly evaluated to clearly address the roles of each component in generation of proton and radical species. The corresponding Gibbs free energy can be calculated from the Rehm-Weller equation (Eq. 6)[58-59]:

$$\Delta G_{ET} = E_{ox}(D) - E_{red}(A) - E_T + C \quad \text{Eq. 6}$$

where $E_{ox}(D)$ refers to the oxidation potential of the electron donor D and E_{red} (A) to the reduction potential of the electron acceptor A. C stands for a coulombic term which is often neglected in polar solvents such as acetonitrile. $E_{red}(IOD^+)$ was measured as -0.70 V / SCE, in agreement with reported values for iodonium salts[60-62]. The reaction was found to be exergonic with ΔG_{ET} = -0.50 eV.

The kinetic of the reaction between ^{3}ITX and IOD^+ was studied by Laser Flash Photolysis (LFP) at 640 nm. By increasing the concentration of IOD^+, ^{3}ITX was found to decay faster. The quenching rate constant $k_q^{3ITX/IOD+}$ was determined from the Stern-Volmer plot as 6.2×10^9 $L.mol^{-1}.s^{-1}$, a value which is in agreement with the high exergonicity of the electron transfer reaction and is similar to the reported values of TX derivative/iodonium salt in acetonitrile.[32,51,61-64] The reduced form of IOD^+ ($IOD^{\bullet}$) is known to decompose itself into an aryl radical and an iodobenzene derivative.[9]

Interestingly, when the triplet state signal at 310 nm and 640 nm was progressively quenched by increasing amounts of IOD^+, a long-lived transient could be detected at 340 nm and around 800 – 850 nm (Figure 1). The electron transfer reaction being exergonic, this new transient was confidently attributed to the radical cation of ITX ($ITX^{\bullet+}$). A similar band has also been reported above 800 nm in the literature.[54] It should be noted that weak transient signal between 400 and 450 nm is traditionally attributed to cation radicals originating from TX derivatives.[62-66] Such a band is also visible on Figure 1, albeit at much lower intensity than those at 340 and 800 – 850 nm. Therefore, it appears reasonable to study the behavior of $ITX^{\bullet+}$ at 340 nm and 800 – 850 nm.

Figure 1. Transient absorption spectrum of ITX in acetonitrile at different times after laser flash in presence of 2×10^{-3} M of IOD^+ (λ_{exc} = 355 nm, 4-5 mJ/pulse). Insert: corresponding decay curves at 340, 440 and 800 nm.

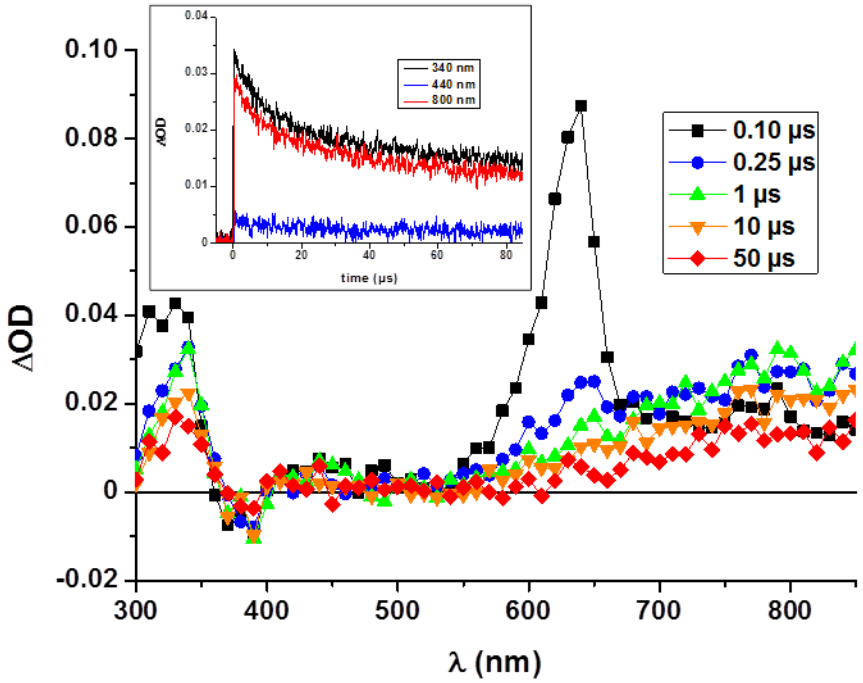

$ITX^{\bullet+}$ can further react with electron donors such as RSH. Considering that $E_{red}(ITX^{\bullet+}) = E_{ox}(ITX)$ and taking into account the value $E_{ox}(RSH)$ = 1.52 V / SCE, the Gibbs free energy of the

reaction was calculated as 0.01 eV. This value indicates that a dark electron transfer reaction between RSH and $ITX^{\bullet+}$ was possible. Therefore, increasing amounts of RSH were introduced in a solution containing ITX and 1.1×10^{-2} M of IOD^{+}. As can be seen on Figure 2, the decay of the long-lived signal of $ITX^{\bullet+}$ was decreased in the presence of RSH. The quenching rate constant was determined to be 1.2×10^{9} $L.mol^{-1}.s^{-1}$ (measured at 340 and 800 nm). This clearly indicates that an electron transfer reaction between $ITX^{\bullet+}$ and RSH occurred, leading to the recovery of ITX ground state. This contention is reinforced by the lower photodegradation of the ITX stationary absorption band in presence of both IOD^{+} and RSH (Figure S2). The oxidized form of RSH ($RSH^{\bullet+}$) is finally expected to deprotonate, yielding a thiyl radical $RS^{\bullet}$ and a proton.

Figure 2. Transient kinetics of $ITX^{\bullet+}$ observed at 340 nm for different IOD^{+} and RSH concentrations in acetonitrile (λ_{exc} = 355 nm, 10 mJ/pulse).

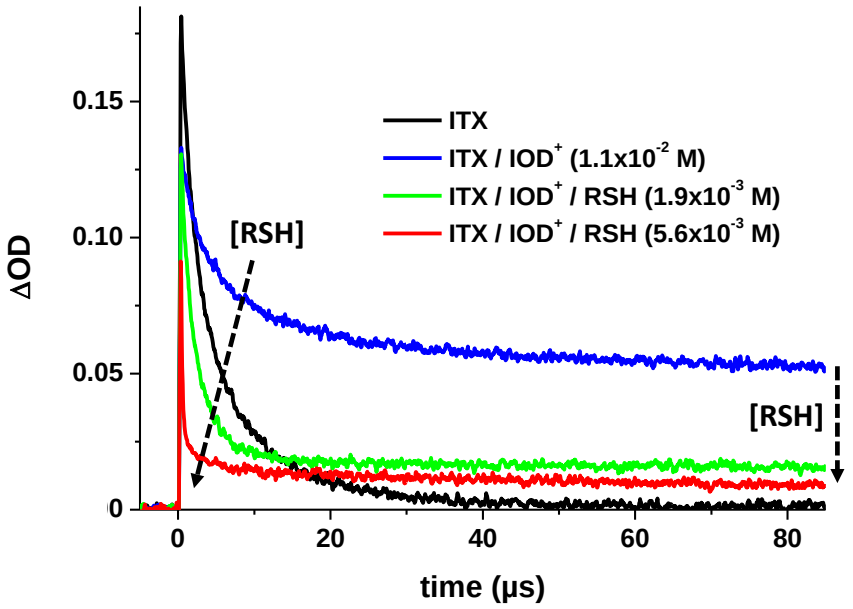

These results clearly reveal the photocyclic behavior of the ITX / IOD^{+} / RSH photoinitiating system. Radicals are produced by the reaction between ^{3}ITX and IOD^{+} followed by a secondary dark reaction between $ITX^{\bullet+}$ and RSH which produces both radicals and protons (Scheme 1). This

combination is expected to initiate both free radical polymerization and sol-gel process, enabling the simultaneous one-pot synthesis of the organic-inorganic hybrid material.

Scheme 1. Mechanism of the ITX / IOD^+ / RSH photocyclic system.

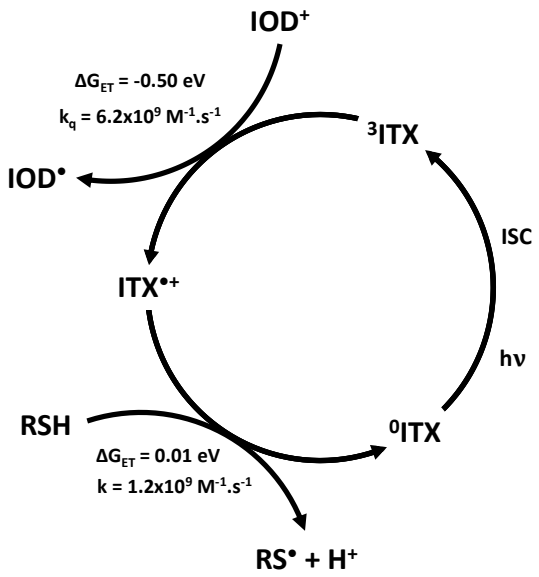

ITX / RSH as primary photoreaction

Due to positive electron transfer Gibbs free energy (0.54 eV), neat electron transfer between ^{3}ITX and RSH can be excluded. One should then consider the well-known photoreduction of aromatic ketones by hydrogen donors (such as thiols), which could occur through coupled electron/proton transfer.[52,67] In the present case, this reaction led to the formation of ketyl ITXH$^\bullet$ and thiyl RS$^\bullet$ radicals. Indeed, ^{3}ITX signal at 640 nm was efficiently quenched when increasing amounts of RSH and the quenching rate constant $k_q^{3ITX/RSH}$ was determined as 1.1×10^9 L.mol^{-1}.s^{-1}. Interestingly, this value is much higher than for aliphatic thiols[47,68], and in the same order of magnitude for aromatic thiols.[52,68] Simultaneously, ITXH$^\bullet$ appeared as a long-lived transient at 420 nm (blue curve on Figure 3), in full agreement with the reported spectrum of ITXH$^\bullet$ in the literature.[47,52,55-

[56,66-67] Ketyl radicals are able to further react with strong electron acceptors.[32,56,69] Therefore, IOD^+ was added to an ITX solution containing 1.7×10^{-1} M of RSH. Kinetics at 420 nm show that the $ITXH^\bullet$ signal was decreased when IOD^+ concentration was increased (Figure 3), resulting in the decrease of the photobleaching signal of ITX at 385 nm (Figure S3). This feature indicates that ITX is efficiently recovered during the reaction. A rate constant of about 10^6 $L.mol^{-1}.s^{-1}$ was measured by a Stern-Volmer treatment of the ketyl radical signal at 420 nm in presence of increasing amounts of IOD^+, in agreement with previous study of a ketyl radical associated to a diphenyliodonium salt in methanol.[69]

Figure 3. Transient kinetics of $ITXH^\bullet$ recorded at 420 nm for various RSH and IOD^+ concentrations in acetonitrile (λ_{exc} = 355 nm, 10 mJ/pulse).

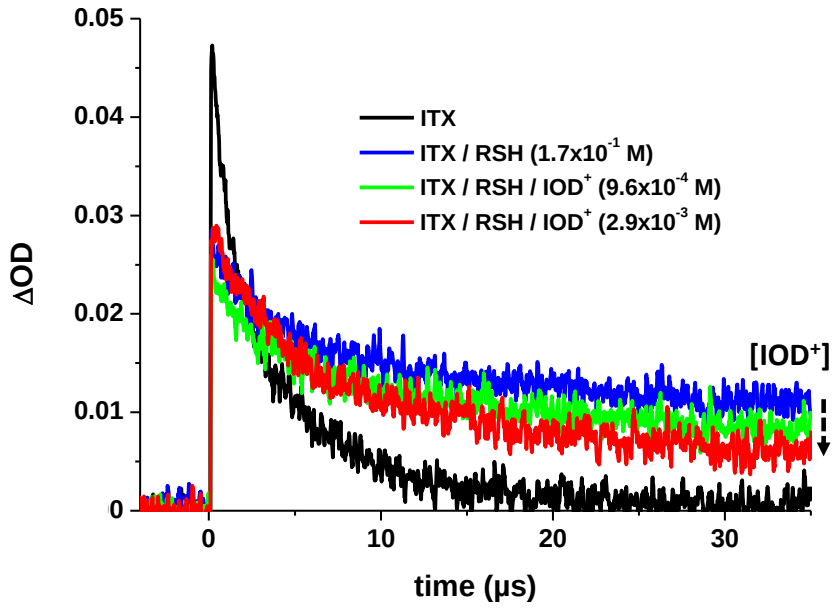

Moreover, it is shown that the photoreaction of ^{3}ITX with RSH and the secondary dark reaction of $ITXH^\bullet$ with IOD^+ also lead to a photocyclic behavior in which radicals and protons are generated, enabling the synthesis of hybrid materials (Scheme 2).

Scheme 2. Mechanism of the ITX / RSH / IOD^+ photocyclic system.

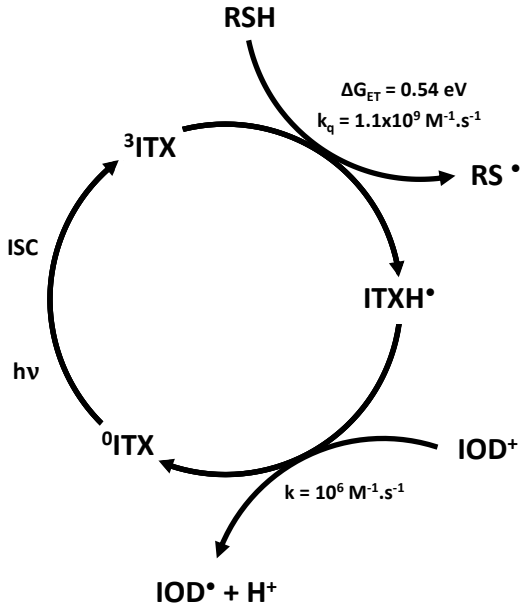

A dual bicyclic initiating system

The previous results showed that the three-component system based on ITX, IOD^+ and RSH can react through two photocyclic processes. Free radicals are produced during the primary and secondary reactions while protons are generated only via the secondary reactions involving the ITX photoproduct (Scheme 3). Therefore, two limiting cases have to be considered, depending on the relative concentrations of IOD^+ and RSH: i) when $k_q^{3ITX/IOD+}[IOD^+] >> k_q^{3ITX/RSH}[RSH]$, the primary photoreaction occurs between ^3ITX and IOD^+ leading to $ITX^{\bullet+}$ which further reacts with RSH (photocycle a) ; ii) when $k_q^{3ITX/IOD+}[IOD^+] << k_q^{3ITX/RSH}[RSH]$, the photoreaction between

^{3}ITX and RSH is favored yielding ITXH$^\bullet$ which is further oxidized by IOD$^+$ (photocycle (b)). It should be noted that when $k_q^{3ITX/IOD^+}[IOD^+] \approx k_q^{3ITX/RSH}[RSH]$, two competitive photocycles take place which are both able to initiate the polymerization, as recently reported for different systems.[70] It is then possible to favor one of the two pathways by finely adjusting the relative concentrations of IOD$^+$ and RSH, knowing the rate constants in the medium.

Scheme 3. Proposed mechanism of reactions for the photocyclic initiating system involving ITX, IOD$^+$ and RSH.

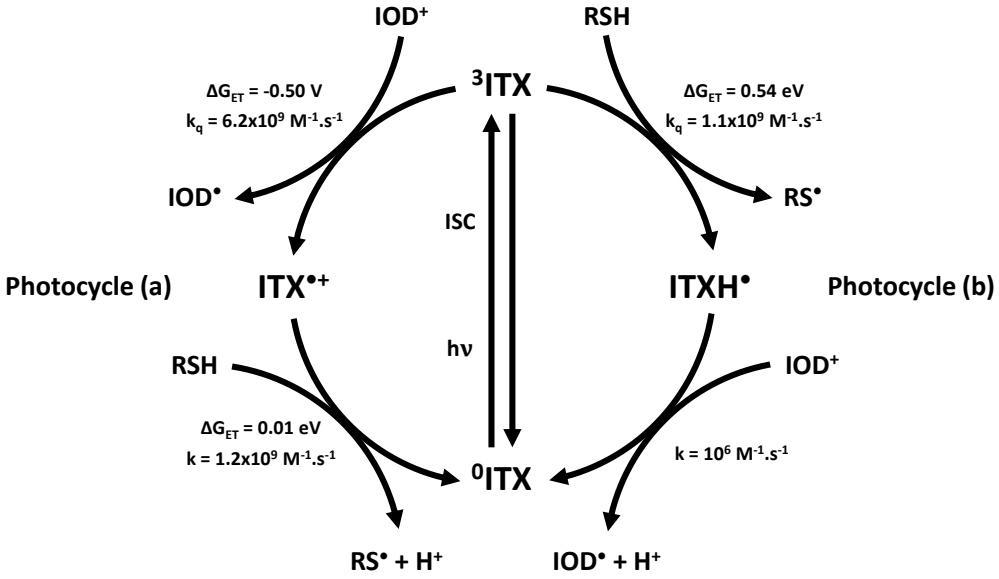

Photogeneration of proton

The two different mechanisms described above show that whatever the photoreaction which primarily occurred (^{3}ITX / IOD$^+$ or ^{3}ITX / RSH), radicals were undoubtedly formed. Protons should also be generated in both cases, which is a hypothesis that needs to be verified. Detection of photogenerated protons at the microsecond scale by LFP had been already reported in the literature.[71] Therefore, in order to prove the photogeneration of acid, we decided to apply a similar

method. It should be noted that the detection of protons generated within the second reaction of a three-component photocyclic system has never been reported up till now.

Quinaldine Red (QR) was used as the molecular probe to detect the release of protons. QR exhibits an absorption maximum at 520 nm, far above from the absorption range of ITX and without overlap with the spectra of the transient species (Figure S4). Preliminary study of a solution of QR in acetonitrile under the same experimental conditions showed that no transient absorption bands appeared in this range upon laser excitation. Moreover, the absence of photochemical reaction between QR and any other components was also assessed.

The basic form of QR is pink in acetonitrile while its protonated form (QRH^+) is colorless (λ_{abs}^{max} = 365 nm). A small amount of QR (< 10^{-5} M) was added to solutions of ITX, IOD^+ and RSH, these two latter being introduced at various concentrations in order to modify the nature of the photocyclic reaction. Because QRH^+ absorbs in the spectral region of the ITX photobleaching, only the evolution of QR at 520 nm was recorded. When introducing increasing concentrations of thiol to a solution of ITX containing 10^{-3} M of IOD^+ (photocycle (a)), a clear photobleaching appeared at 520 nm (Figure 4a) which is attributed to the disappearance of QR to form QRH^+. UV-vis spectra were recorded before and after laser irradiation (Figure 4b), confirming the decrease of the 520 nm band of QR after laser excitation, and the growing shoulder at 365 nm was attributed to QRH^+.

Figure 4. a) Transient kinetics measured at 800 nm ($ITX^{\bullet+}$) and 520 nm (QR bleaching) in the presence of QR at 10^{-3}M of IOD^+ and various RSH concentrations in acetonitrile (λ_{exc} = 355 nm, 10 mJ/pulse). b) Corresponding UV-vis absorption spectra in acetonitrile before and after laser irradiation.

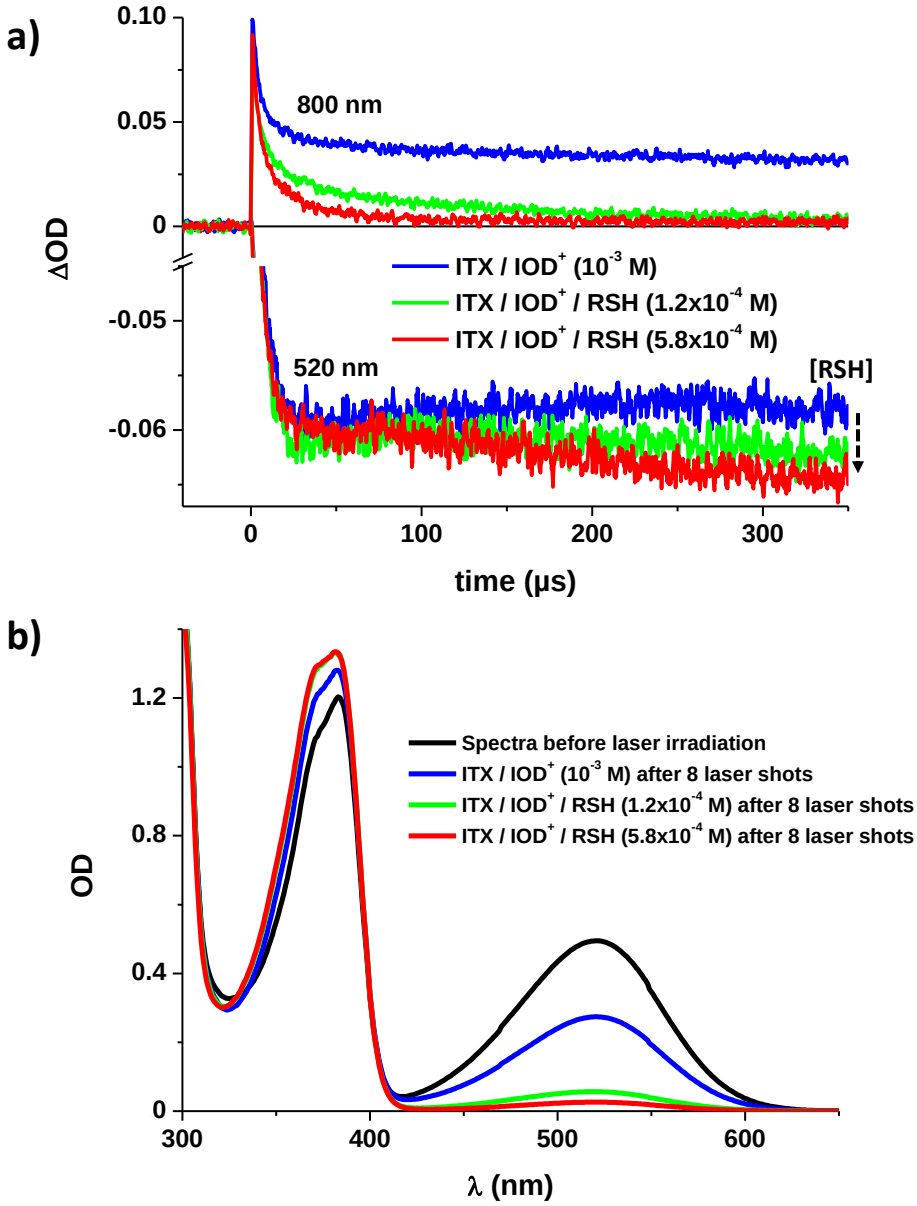

The same behavior is also observed at 520 nm for photocycle (b) (Figure 5a). UV-visible spectra show a shoulder similar to that previously observed (Figure 5b). It can be conclude that the photogeneration of acid actually occurs through the two photocyclic pathways.

Figure 5. Transient kinetics recorded at 420 nm ($ITXH^{\bullet}$) and 520 nm (QR bleaching) in the presence of QR at 1.7×10^{-1} M of RSH and various IOD^{+} concentrations in acetonitrile (λ_{exc} = 355 nm, 10 mJ/pulse). b) Corresponding UV-vis absorption spectra in acetonitrile before and after laser irradiation.

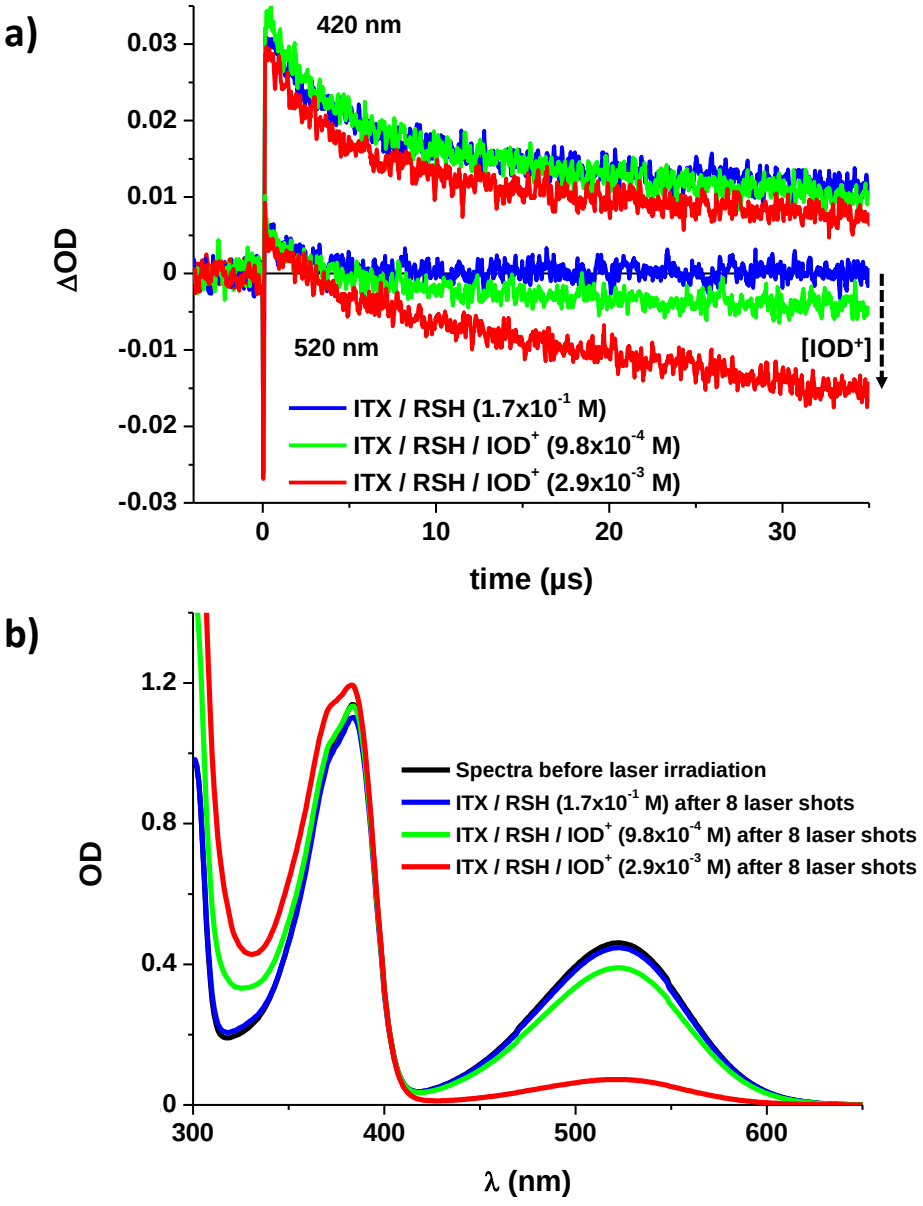

UV-vis spectra shown in Figures 4 and 5 were obtained with the same number of laser pulses. However, it clearly appears that the photolysis signal of QR at 520 nm was lower for photocycle

(a) as compared to (b) (Figures 4 and 5). It suggests that the photoacid generation efficiency is higher when ^{3}ITX first reacted with IOD^+. In order to quantify this difference in reactivity, proton production quantum yield Φ_{H+} was estimated by steady-state spectroscopic measurements. Values of $\Phi_{H+} = 0.12$ (standard deviation $\sigma = 0.012$) and 0.017 ($\sigma = 0.003$) for photocycles (a) and (b), respectively, confirmed the differences observed by LFP. Pathway (a) is then almost 7-times more efficient than pathway (b). This may be explained by a better reactivity of $ITX^{\bullet+}$ with RSH compared to $ITXH^{\bullet}$ with IOD^+ in acetonitrile, as attested by the rate constants of these reactions (1.2×10^9 and 10^6 $M^{-1}.s^{-1}$ respectively).

Application of dual bicyclic initiating system for synthesis of organic-inorganic material

The ability of the bicyclic system to generate initiating radicals and protons simultaneously can be employed to perform simultaneously a free radical photopolymerization (FRP) and a photoacid catalyzed sol-gel reaction (PSG) under LED at 395 nm. A difunctional methacrylate monomer (SR348C) was selected for attesting radical initiation of organic polymerization and a poly(dimethoxysiloxane) sol-gel precursor (PDMOS) was used for proton-catalyzed photoinduced sol-gel process (Chart 1).

The diffusion rate constant k_{diff} in these monomers can be estimated according to the Stokes-Einstein equation.[72] Values of 5×10^6 and 10^9 $M^{-1}.s^{-1}$ were found, respectively, for SR348C and PDMOS. Because $k_q^{ITX/IOD+}$ and $k_q^{ITX/RSH}$ measured in acetonitrile are both greater than these values, they can be considered as equal in SR348C and PDMOS. Therefore, the two photochemical pathways were differentiated by introducing ten times more (in mol%, based on the monomer) of one of the co-initiators with respect to the second one. In SR348C, the dark reaction rate constants for photocycles (a) and (b) are greater than (or almost equal to) k_{diff} and these reactions are also

diffusion-limited. The same holds true for pathway (a) in PDMOS. However, the dark reaction in pathway (b) is clearly not limited by the diffusion as $k^{ITXH•/IOD+}$ is lower than k_{diff}.

For sake of comparison, the two-component systems ITX/IOD^+ or ITX/RSH were first analyzed. The conversion profiles of the acrylate monomer during light exposure under air are displayed in Figure 6. Final conversions and maximum polymerization rates are collected in Table 2. Final conversions were found to be low for these two-component systems, most probably because of a relatively low production of radicals. In addition, aryl radicals produced from the interaction ITX/IOD^+ are very sensitive to molecular oxygen, leading to inactive peroxy radicals ($k_{O2} \approx 10^{10}$ $M^{-1}.s^{-1}$ [73], also limited to k_{diff}). On the contrary, thiyl radicals are known to overcome oxygen inhibition in free radical polymerization.[14-15,74-75] This could explain the difference between the two-component systems.

Figure 6. Acrylate double bonds conversion profiles of SR348C (measured at 1310 cm^{-1}) using various combinations of ITX, IOD^+ and RSH (λ_{irr} = 395 nm, 20 $mW.cm^{-2}$).

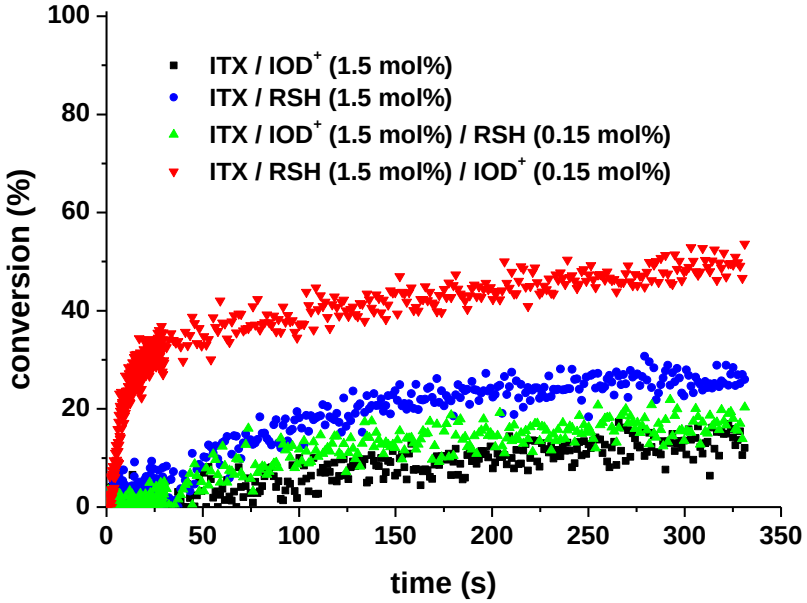

Introduction of a third component in the PISs improved the FRP performances when compared to the corresponding two-component systems by virtue of the photocyclic behaviour. This can be explained by two facts. First, additional initiating radicals are generated through the dark secondary reaction of the photocycles. Secondly, ground state ITX is recovered during the photocycle and can further absorb the light, leading to longer availability of the photoinitiator in the formulation.[70] Moreover, it clearly appears that photocycle (b) gave better results than (a). This effect may be attributed to the better efficiency of photocycle (b) to lead to the recovery of ITX. Therefore, more ITX is still available for light absorption, leading to an increased reactivity of photocycle (b).

Table 2. Final conversion, maximum conversion rate R_c^{max} and final hydrolysis ratio for the different photoinitiating systems.

System	SR348C	PDMOS	SR348C/PDMOS (20/80 mol%)	
	Conversion (%) / R_c^{max} (s^{-1})	**Hydrolysis ratio (%)**	**Conversion (%) / R_c^{max} (s^{-1})**	**Hydrolysis ratio (%)**
ITX/IOD$^+$ (1.5 mol%)	14 / 0.7	100	/	/
ITX/RSH (1.5 mol%)	27 / 0.9	29	/	/
ITX/IOD$^+$ (1.5 mol%)/ RSH (0.15 mol%) = photocycle (a)	17 / 0.8	100	34 / 16	100
ITX/RSH (1.5 mol%)/ IOD$^+$ (0.15 mol%) = photocycle (b)	50 / 10.5	100	38 / 6	71

The efficiency of the photosol-gel reaction was studied by monitoring the conversion of the $SiOCH_3$ groups of PDMOS. In the absence of IOD^+, only 29% of the alkoxy functions were hydrolyzed after 200 s without IOD^+ (Figure 7). This 29% hydrolysis ratio observed in presence

of only RSH may be directly due to residual water present in the reaction medium. By contrast, the presence of IOD^+ led to fast and efficient hydrolysis.

Figure 7. Hydrolysis ratio profiles of PDMOS (recorded at 2848 cm^{-1}) using various combinations of ITX, IOD^+ and RSH (λ_{irr} = 395 nm, 20 $mW.cm^{-2}$).

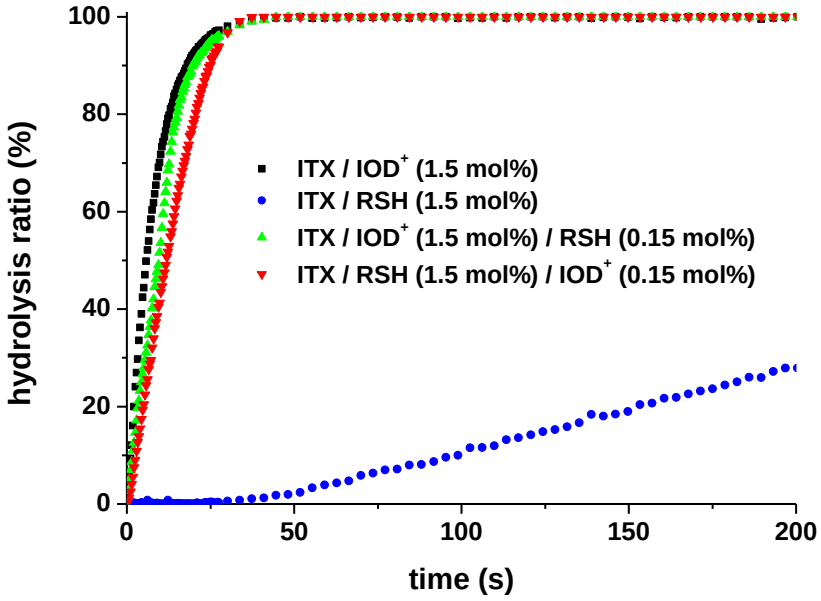

Any of the two photocycles (a) or (b) led to a fast and efficient hydrolysis. In fact, the production of protons after reaction of ^3ITX with RSH relies on an electron transfer from $ITXH^\bullet$ to IOD^+ followed by a rapid deprotonation of $ITXH^+$ (photocycle (b)). In the case of photocycle (a), any hydrogen donor (such as water or CH_3OH liberated from PDMOS during the process) can react with $ITX^{\bullet+}$ to produce a proton in photocycle (a). This was the reason why two- and three-component systems present similar results for pathway (a).

Comparing the two photocycles, it appears that pathway (a) led to a faster hydrolysis of the PDMOS. This can be related to the value of acid quantum yield of 0.12 determined previously. As

the PDMOS is a low-viscous liquid ($k_{diff} \approx 10^9$ $M^{-1}.s^{-1}$), the secondary dark reaction between $ITX^{\bullet+}$ and RSH is quite efficient and occurs with a high rate constant ($k^{ITX\bullet+/RSH} = k_{diff}$).

Finally, the ability to induce concomitant reactions was studied for a 20/80 mol% SR348C/PDMOS mixture under LED irradiation (Figure 8). Photocycle (a) led to a fast hydrolysis of PDMOS while photocycle (b) is in favor of a better methacrylate polymerization. Interestingly, the final conversion was found higher in the case of the hybrid than for the pure SR348C for pathway (a) (40% vs. 17%). The presence of low-viscous PDMOS increases the rate of polymerization of SR348C. However, the simultaneous conversion of PDMOS rapidly increases the viscosity, thereby limiting the final conversion of SR348C. On the opposite, the low acid quantum yield of photocycle (b) allows good conversion of methacrylate, although at slow rate.

These results nicely illustrate the conclusion obtained from the previous mechanistic study, and the successful synthesis of both organic and inorganic networks demonstrates the simultaneous generation of free radicals and protons through the bicyclic photoinitiating system. Moreover, the ability of this system to mediate the one-pot light-induced synthesis of organic-inorganic hybrids has also been clearly established.

Figure 8. Acrylate double bonds conversion profiles of SR348C (▲) and hydrolysis ratio of PDMOS (●) in a 20/80 mol% mixture of SR348C/PDMOS with photocyclic initiating systems (green ITX / IOD^+ / RSH – 1.5 / 0.15 mol% and red ITX / RSH / IOD^+ – 1.5 / 0.15 mol%) (λ_{irr} = 395 nm, 20 $mW.cm^{-2}$).

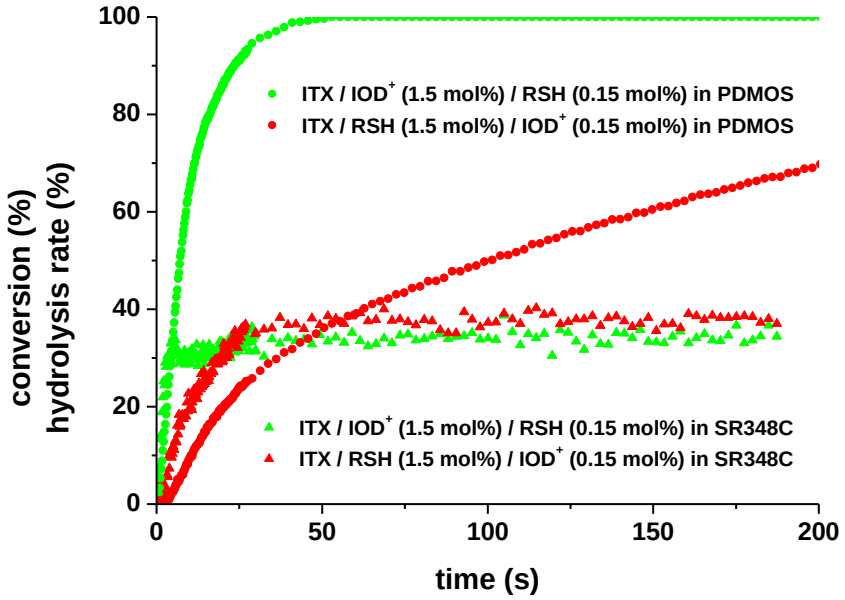

Conclusions

The photochemical mechanism of a new bicyclic photoinitiating system for concomitant synthesis of organic-inorganic hybrid materials under LED irradiation was elucidated. Triplet state of ITX can primary react with an iodonium salt IOD^+ or a tetrafunctional thiol RSH, and the ITX photoproduct ($ITX^{\bullet+}$ or $ITXH^{\bullet}$) further reacts (respectively RSH and IOD^+) to increase the formation of acid and radicals. The proton generation was assessed at the microsecond scale with a proton-sensitive probe, and the acid quantum yield was also calculated. Free radical photopolymerization of dimethacrylate monomer and sol-gel reaction were performed using this photocyclic initiating system. Polymerization results were in good agreement with the conclusions drawn from mechanistic study. Finally, a hybrid material was successfully produced, attesting the dual initiating character of the bicyclic system.

Supporting Information. Transient absorption spectra of ITX at different time after laser flash; UV-vis absorption spectra of ITX / IOD^+ and ITX / IOD^+ / RSH systems before and after laser irradiation; photobleaching kinetics at 385 nm of ITX, ITX / RSH and ITX / RSH / IOD^+ systems; UV-vis absorption spectra of protonated and non-protonated Quinaldine Red. This material is available free of charge via the Internet at http://pubs.acs.org.

Acknowledgement

The authors would like to thank Mäder and ANR for funding the DeepCure project (#ANR-13-CHIN-0004-01)

References

(1) Ciamician, G. The Photochemistry of the Future. *Science* **1912**, *36*, 385–394.

(2) Fouassier, J-P. In *Photoinitiation, Photopolymerization, and Photocuring: Fundamentals and Applications*; Hanser/Gardner Publications: Munich, Germany, 1995.

(3) Allonas, X.; Croutxé-Barghorn, C.; Fouassier, J-P.; Lalevée, J.; Malval, J-P.; Morlet-Savary, F. *Lasers in the Photopolymer Area* in *Lasers in Chemistry, Influencing Matter* (edited by M. Lackner); Wiley-VCH, Weinheim, Germany, 2008.

(4) Schnabel, W. *Polymers and Light: Fundamentals and Technical Applications*; Wiley-VCH Verlag Gmbh: Weinheim, Germany, 2007.

(5) Odian, G. *Principles of Polymerization – Fourth Edition*; John Wiley & Sons, Inc: Hoboken, USA, 2004.

(6) Decker, C. UV-Radiation Curing Chemistry. *Pigm. Resin Technol.* **2001**, *30*, 278–286.

(7) Yagci, Y.; Jockusch, S.; Turro, N. J. Photoinitiated Polymerization: Advances, Challenges, and Opportunities. *Macromolecules* **2010**, *43*, 6245–6260.

(8) Ibrahim, A. ; Di Stefano, L. H. ; Tarzi, O. ; Tar, H. ; Ley, C. ; Allonas, X. High-Perfomance Photoinitiating Systems for Free Radical Photopolymerization. Application to Holographic Recording. *Photochem. Photobiol.* **2013**, *89*, 1283–1290.

(9) Crivello, J. V. *Cationic Polymerization – Iodonium and Sulfonium Salt Photoinitiators* in the series *Advances in Polymer Science*; Springer-Verlag: Berlin, Germany, 1984.

(10) Yagci, Y.; Reetz, I. Externally Stimulated Initiator Systems for Cationic Polymerization. *Prog. Polym. Sci.* **1998**, *23*, 1485–1538.

(11) Crivello, J. V. The Discovery and Development of Onium Salt Cationic Photoinitiators. *J. Polym. Sci. A: Pol. Chem.* **1999**, *37*, 4241–4254.

(12) Sangermano, M.; Razza, N.; Crivello, J. V. Cationic UV-Curing: Technology and Applications. *Macromol. Mat. Eng.* **2014**, *299*, 775–793.

(13) Salmi, H.; Allonas, X.; Ley, C.; Defoin, A.; Ak, A. Quaternary Ammonium Salts of Phenylglyoxylic Acid as Photobase Generators for Thiol-Promoted Epoxide Photopolymerization. *Polym. Chem.* **2014**, *5*, 6577–6583.

(14) Hoyle, C. E.; Lee, T. Y.; Roper, T. Thiol-Enes: Chemistry of the Past with Promise for the Future. *J. Polym. Sci. A: Pol. Chem.* **2004**, *42*, 5301–5338.

(15) Hoyle, C. E.; Bowman, C. N. Thiol-Ene Click Chemistry. *Ang. Chem. Int. Ed.* **2010**, *49*, 1540–1573.

(16) Tasdelen, M. A.; Yagci, Y. Light-Induced Click Reactions. *Ang. Chem. Int. Ed.* **2013**, *52*, 5930–5938.

(17) Tasdelen, M. A.; Kiskan, B.; Yagci, Y. Externally Stimulated Click Reactions for Macromolecular Syntheses. *Prog. Polym. Sci.* **2016**, *52*, 19–78.

(18) Belon, C. ; Chemtob, A. ; Croutxé-Barghorn, C. ; Rigolet, S.; Le Houérou, V. ; Gauthier, C. Combination of Radical and Cationic Photoprocesses for the Single-Step Synthesis of Organic-Inorganic Hybrid Films. *J. Polym. Sci. A: Pol. Chem.* **2010**, *48*, 4150–4158.

(19) Nishibayashi, M.; Yoshida, H.; Uenishi, M.; Kanezashi, M.; Nagasawa, H.; Yoshioka, T.; Tsuru, T. Photo-Induced Sol-Gel Processing for Low-Temperature Fabrication of High-Performance Silsesquioxane Membranes for Use in Molecular Separation. *Chem. Commun.* **2015**, *51*, 9932–9935.

(20) Crivello, J. V.; Mao, Z. B. Preparation and Cationic Photopolymerization of Organic-Inorganic Hybrid Matrixes. *Chem. Mat.* **1997**, *9*, 1562–1569.

(21) Chemtob, A.; Versace, D-L.; Belon, C.; Croutxé-Barghorn, C.; Rigolet, S. Concomitant Organic-Inorganic UV-Curing Catalyzed by Photoacids. *Macromolecules* **2008**, *41*, 7390–7398.

(22) Ni, L.; Chemtob, A.; Croutxé-Barghorn, C.; Moreau, N.; Bouder, T.; Chanfreau, S.; Pébère, N. Direct-to-Metal UV-Cured Hybrid Coating for the Corrosion Protection of Aircraft Aluminium Alloy. *Corros. Sci.* **2014**, *89*, 242–249.

(23) Dietliker, K. *A Compilation of Photoinitiators Commercially Available for UV Today*; Sita Technology Limited: Edinburgh/London, U.K., 2002.

(24) Green, W. A. *Industrial Photoinitiators – A Technical Guide*; CRC Press: Boca Raton, USA, 2010.

(25) Fouassier, J-P.; Morlet-Savary, F.; Lalevée, J.; Allonas, X.; Ley, C. Dyes as Photoinitiators or Photosensitizers of Polymerization Reactions. *Materials* **2010**, *3*, 5130–5142.

(26) Fouassier, J. P.; Allonas, X.; Burget, D. Photopolymerization Reactions Under Visible Lights: Principle, Mechanisms and Examples of Applications. *Prog. Org. Coat.* **2003**, *47*, 16–36.

(27) Shi, S.; Karasu, F.; Rocco, C.; Allonas, X.; Croutxé-Barghorn, C. Photoinitiating Systems for LED-Cured Interpenetrating Polymer Networks. *J. Photopolym. Sci. Technol.* **2015**, *28*, 31–35.

(28) Shao, J.; Huang, Y.; Fan, Q. Visible Light Initiating Systems for Photopolymerization: Status, Development and Challenges. *Polym. Chem.* **2014**, *5*, 4195–4210.

(29) Gómez, M. L.; Previtali, C. M.; Montejano, H. A. Two and Three-Component Visible Light Photoinitiating Systems for Radical Polymerization Based on Onium Salts: An Overview of Mechanistic and Laser Flash Photolysis. *Int. J. Photoenergy* **2012**, *2012*, 1–9.

(30) Shi, S.; Croutxé-Barghorn, C.; Allonas, X. Photoinitiating Systems for Cationic Photopolymerization: Ongoing Push Toward Long Wavelengths and Low Light Intensities. *Prog. Polym. Sci.* **2016**, DOI:10.1016/j.progpolymsci.2016.09.007.

(31) Crivello, J. V.; Lam, J. H. W. Dye-Sensitized Photoinitiated Cationic Polymerization. *J. Polym. Sci. A: Pol. Chem.* **1978**, *16*, 2441–2451.

(32) Fouassier, J-P.; Burr, D.; Crivello, J. V. Photochemistry and Photopolymerization Activity of Diaryliodonium Salts. *Pure Appl. Chem.* **1994**, *31*, 677–701.

(33) Dadashi-Silab, S.; Aydogan, C.; Yagci, Y. Shining a Light on an Adaptable Photoinitiator: Advances in Photopolymerization Initiated by Thioxanthones. *Polym. Chem.* **2015**, *6*, 6595–6615.

(34) Soppera, O.; Croutxé-Barghorn, C.; Lougnot, D. J. New Insights into Photoinduced Processes in Hybrid Sol–Gel Glasses Containing Modified Titanium Alkoxides. *New J. Chem.* **2001**, *25*, 1006–1014.

(35) Chemtob, A.; Belon, C.; Croutxé-Barghorn, C.; Brendlé, J.; Soulard, M.; Rigolet, S.; Le Houérou, V.; Gauthier, C. Bridged Polysilsesquioxane Films *Via* Photoinduced Sol-Gel Chemistry. *New J. Chem.* **2010**, *34*, 1068–1072.

(36) De Paz, H.; Chemtob, A.; Croutxé-Barghorn, C.; Le Nouen, D.; Rigolet, S. Insights into Photoinduced Sol-Gel Polymerization: An *in Situ* Infrared Spectroscopy Study. *J. Phys. Chem. B* **2012**, *116*, 5260–5268.

(37) Shi, S.; Allonas, X.; Croutxé-Barghorn, C.; Chemtob, A. Activation of the Sol-Gel Process by Visible Light-Emitting Diodes (LEDs) for the Synthesis of Inorganic Films. *New J. Chem.* **2015**, *39*, 5686–5693.

(38) Melhuish, W. H. Quantum Efficiencies of Fluorescence of Organic Substances: Effect of Solvent and Concentration of the Fluorescent Solute. *J. Phys. Chem.* **1961**, *65*, 229–235.

(39) Rosspeintner, A.; Angulo, G.; Weiglhofer, M.; Landgraf, S.; Grampp, G. Photophysical Properties of 2-6,dicyano-N,N,N',N'-tetramethyl-*p*-phenylenediamine. *J. Photochem. Photobiol. A.* **2006**, *183*, 225–235.

(40) Christmann, J.; Ibrahim, A.; Charlot, V.; Croutxé-Barghorn, C.; Ley, C.; Allonas, X. Elucidation of the Key Role of $(Ru(bpy)_3)^{2+}$ in Photocatalyzed RAFT Polymerization. *Chem. Phys. Chem.* **2016**, *17*, 2309–2314.

(41) Dietlin, C.; Allonas, X.; Defoin, A.; Fouassier, J. P. Theoretical and Experimental Study of the Norrish I Photodissociation of Aromatic Ketones. *Photochem. Photobiol. Sci.* **2008**, *7*, 558–565.

(42) Jacques, P.; Burget, D.; Allonas, X. On the Quantitative Appraisal of the Free-Energy Change ΔG_{ET} in Photoinduced Electron-Transfer. *New J. Chem.* **1996**, *20*, 933–937.

(43) Allonas, X.; Fouassier, J. P.; Kaji, M.; Murakami, Y. Excited State Processes in a Four-Component Photosensitive System Based on a Bisimidazole Derivative. *Photochem. Photobiol. Sci.* **2003**, *2*, 224–229.

(44) Suzuki, S.; Allonas, X.; Fouassier, J-P.; Urano, T.; Takahara, S.; Yamaoka, T. Interaction Mechanism in Pyrromethene Dye/Photoacid Generator Photosensitive System for High Speed Photopolymer. *J. Photochem. Photobiol. Pol. Chem.* **2006**, *181*, 60–66.

(45) Decker, C.; Moussa, K. Real-Time Kinetic Study of Laser-Induced Polymerization. *Macromolecules* **1989**, *22*, 4455–4462.

(46) Ibrahim, A.; Maurin, V.; Ley, C.; Allonas, X.; Croutxe-Barghorn, C.; Jasinski, F. Investigation of Termination Reactions in Free Radical Photopolymerization of UV Powder Formulations. *Eur. Polym. J.* **2012**, *48*, 1475–1484.

(47) Amirzadeh, G.; Schnabel, W. On the Photoinitiation of Free Radical Polymerization – Laser Flash Photolysis Investigations on Thioxanthone Derivatives. *Makromol. Chem.* **1981**, *182*, 2821–2835.

(48) Steidl, L.; Jhaveri, S. J.; Ayothi, R.; Sha, J.; McMullen, J. D.; Ng, S. Y. C.; Zipfel, W. R.; Zentel, R.; Ober, C. K. Non-Ionic Photo-Acid Generators for Applications in Two-Photon Lithography. *J. Mater. Chem.* **2009**, *19*, 505–513.

(49) Segurola, J.; Allen, N. S.; Edge, M.; Parrondo, A.; Roberts, I. Photocuring Activity of Several Commercial, Near UV Activated Photoinitiated in Clear and Pigmented Systems. *J. Coat. Technol.* **1999**, *71*, 61–67.

(50) Lalevée, J.; Blanchard, N.; Tehfe, M. A.; Fries, C.; Morlet-Savary, F.; Gigmes, D.; Fouassier, J-P. New Thioxanthone and Xanthone photoinitiators Based on Sylil Radical Chemistry. *Polym. Chem.* **2011**, *2*, 1077–1084.

(51) Manivannan, G.; Fouassier, J-P. Primary Processes in the Photosensitized Polymerization of Cationic Monomers. *J. Polym. Sci. A: Pol. Chem.* **1991**, *29*, 1113–1124.

(52) Andrzejewska, E.; Zych-Tomkowiak, D.; Andrzejewski, M.; Hug, G. L.; Marciniak, B. Heteroatomic Thiols as Co-initiators for Type II Photoinitiating Systems Based on Camphorquinone and Isopropylthioxanthone. *Macromolecules* **2006**, *39*, 3777–3785.

(53) Zhu, Q. Q.; Fink, M.; Seitz, F.; Schneider, S.; Schnabel, W. On the Photolysis of bis[2-(*o*-Chlorophenyl)-4,5-diphenylimidazole] sensitized by 2-Isopropylthioxanthone or Michler's Ketone. *J. Photochem. Photobiol. A* **1991**, *59*, 255–263.

(54) Pohlers, G.; Scaiano, J. C.; Step, E.; Sinta, R. Ionic vs Free Radical Pathways in the Direct and Sensitized Photochemistry of 2-(4'-Methoxynaphthyl)-4,6-bis(trichloromethyl)-1,3,5-triazine: Relevance for Photoacid Generation. *J. Am. Chem. Soc.* **1999**, *121*, 6167–6175.

(55) Fouassier, J-P.; Allonas, X.; Lalevée, J.; Visconti, M. Radical Polymerization Activity and Mechanistic Approach in a New Three-Component Photoinitiating System. *J. Polym. Sci. A: Pol. Chem.* **2000**, *38*, 4531–4541.

(56) Charlot, V.; Ibrahim, A.; Allonas, X.; Croutxé-Barghorn, C.; Delaite, C. Photopolymerization of Methyl Methacrylate: Effects of Photochemical and Photonic Parameters on the Chain Length. *Polym. Chem.* **2014**, *5*, 6236–6243.

(57) Dossot, M.; Sylla, M.; Allonas, X.; Merlin, A.; Jacques, P.; Fouassier, J. P. Role of phenolic derivatives in photopolymerization of an acrylate coating. *J. Appl. Polym. Sci.* **2000**, *78*, 2061–2074.

(58) Rehm, D.; Weller, A. Kinetik und Mechanismus der elektronbertragung bei der fluoreszenzloshung in acetonitril. *Ber. Bunsenges. Phys. Chem.* **1969**, *73*, 834–839.

(59) Rehm, D.; Weller, A. Kinetics of Fluorescence Quanching by Electron and H-Atom Transfer. *Isr. J. Chem.* **1970**, *8*, 259–271.

(60) Bachofner, H. E.; Beringer, F. M.; Meites, L. Diaryliodonium Salts V. The Electroreduction of Diphenyliodonium Salts. *J. Am. Chem. Soc.***1958**, *80*, 4269–4274.

(61) Timpe, H. J.; Kronfeld K. P.; Lammel, U. Excited States of Ketones as Electron Donors – Ketone-Iodonium Salt Systems as Photoinitiators for Radical Polymerization. *J. Photoch. Photobio. A* **1990**, *52*, 111–122.

(62) Kunze, A.; Müller, U.; Tittes, K.; Fouassier, J-P.; Morlet-Savary, F. Triplet Quenching by Onium Salts in Polar and Nonpolar Solvents. *J. Photochem. Photobiol. A.* **1997**, *110*, 115–122.

(63) Fouassier, J-P.; Burr, D.; Crivello, J. V. Time-Resolved Laser Spectroscopy of the Sensitized Photolysis of Iodonium Salts. *J. Photochem. Photobiol. A* **1989**, *49*, 317–324.

(64) Toba, Y.; Usui, Y.; Alam, M. M.; Ito, O. Onium Butyltriphenylborates as Donor-Acceptor Initiators for Sensitized Photopolymerizations of Vinyl Monomer. *Macromolecules* **1998**, *31*, 6022–6029.

(65) Manivannan, G.; Fouassier, J-P.; Crivello, J. V. Chlorothioxanthone-Onium Salts: Efficient Photoinitiators of Cationic Polymerization. *J. Polym. Sci. A: Pol. Chem.* **1992**, *30*, 1999–2001.

(66) Rodrigues, M. R.; Neumann, M. G. Mechanistic Study of Tetrahydrofuran Polymerization Photoinitiated by a Sulfonium/Thioxanthone System. *Macromol. Chem. Phys.* **2001**, *202*, 2776–2782.

(67) Yates, S. F.; Schuster, G. B. Photoreduction of Triplet Thioxanthone by Amines: Charge Transfer Generates Radicals That Initiate Polymerization of Olefins. *J. Org. Chem.* **1984**, *49*, 3349–3356.

(68) Lalevée, J.; Morlet-Savary, F.; El Roz, M.; Allonas, X.; Fouassier, J-P. Thiyl Radical Generation in Thiol or Disulfide Containing Photosensitive Systems. *Macromol. Chem. Phys.* **2009**, *210*, 311–319.

(69) Erddalane, A.; Fouassier, J-P.; Morlet-Savary, F.; Takimoto, Y. Efficiency and Excited State Processes in a Three-Component System, Based on Thioxanthene Derived Dye/Amine/Additive, Usable in Photopolymer Plates. *J. Polym. Sci. A: Pol. Chem.* **1996**, *34*, 633–642.

(70) Ley, C.; Christmann, J.; Ibrahim, A.; Di Stefano, L. H.; Allonas, X. Tailoring of Organic Dyes with Oxidoreductive Compounds to Obtain Photocyclic Radical Generator Systems Exhibiting Photocatalytic Behavior. *Beilstein J. Org. Chem.* **2014**, *10*, 936–947.

(71) Pohlers, G.; Scaiano, J. C. A Novel Photometric Method for the Determination of Photoacid Generation Efficiencies Using Benzothiazole and Xanthene Dyes as Acid Sensors. *Chem. Mater.* **1997**, *9*, 3222–3230.

(72) Ibrahim, A.; Allonas, X.; Ley, C.; Kawamura, K.; Berneth, H.; Bruder, F. K.; Fäcke, T.; Hagen, R.; Hönel, D.; Rölle, T. High Performance Photoinitiating Systems for Holography Recording: Need for a Full Control of Primary Processes. *Chem. Eur. J.* **2014**, *20*, 15102–15107.

(73) Sommeling, P. M.; Mulder, P.; Louw, R.; Avila, D. V.; Lusztyk, J.; Ingold, K. U. Rate of Reaction of Phenyl Radicals with Oxygen in Solution and in the Gas Phase. *J. Phys. Chem.* **1993**, *97*, 8361–8364.

(74) Karash, M. S.; Nudenberg, W.; Mantell, G. J. Reactions of Atoms and Free Radicals in Solution. XXV. The Reactions of Olefins with Mercaptans in the Presence of Oxygen. *J. Org. Chem.* **1951**, *16*, 524–532.

(75) O'Brien, A. K.; Cramer, N. B.; Bowman, C. N. Oxygen Inhibition in Thiol-Acrylate Photopolymerizations. *J. Polym. Sci. A: Pol. Chem.* **2006**, *44*, 2007–2014.

Table of Contents Graphic and Synopsis

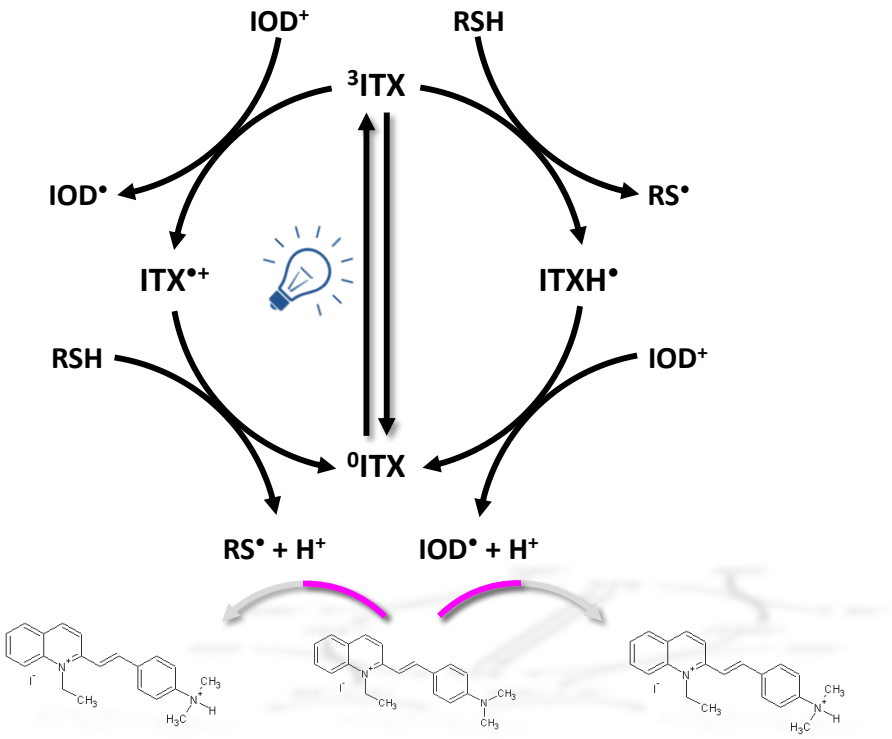

AUTHOR INFORMATION

Corresponding Author

* xavier.allonas@uha.fr

† **Present address:**

Key Laboratory of Synthetic and Natural Functional Molecule Chemistry of Ministry of Education and College of Chemistry & MaterialScience, Northwest University, Xi'an 710069, PR China

Author Contributions

The manuscript was written through contributions of all authors. All authors have given approval to the final version of the manuscript. ‡These authors contributed equally. (match statement to author names with a symbol)